

Linear and non-linear QSAR models on platinum (II) anticancer drugs with N-donor ligands

Robabeh Sayyadi Kord Abadi*^a, Asghar Alizadehdakhel^b & Fereshteh Moosapour^a

^aDepartment of Chemistry, Rasht Branch, Islamic Azad University, Rasht, Iran

^bDepartment of Chemical Engineering, Rasht Branch, Islamic Azad university, Rasht, Iran
E-mail: sayyadi@iaurasht.ac.ir

Received 4 April 2016; accepted (revised) 6 February 2017

This research presents a quantitative structure-activity relationship (QSAR) of IC50 values of Platinum(II) derivatives. Twenty one different platinum(II) anticancer derivatives have been selected as a sample set and the geometry of the complexes are optimized using Gaussian 03W. The activity of the 21 different Platinum(II) derivatives is estimated by means of multiple linear regression (MLR), artificial neural network (ANN), simulated annealing (SA) and genetic algorithm (GA) techniques. These methods are also utilized to select the most efficient subsets of descriptors in a cross-validation procedure for non-linear $-\log(\text{IC}_{50})$ prediction. The results obtained using the GA-ANN have been compared with those obtained using MLR-MLR, MLR-ANN, SA-ANN and GA-ANN approaches. A high predictive ability has been observed for the MLR-MLR, MLR-ANN, SA-ANN, MLR-GA and GA-ANN models, with root mean sum square errors (RMSE) of 0.127, 0.013, 0.011, 0.0125 and 0.0099, respectively (N=21). The results obtained using the GA-ANN method indicate that the activity of the derivatives of Platinum complexes depends on different parameters such as Mor9v, RDF140v and G2e descriptors. In summary, a comparison of the quality of ANN with different MLR methods shows that ANN has a better predictive ability.

Keywords: Platinum complexes, antitumor drugs, QSAR, MLR

Platinum (II) complex, namely cisplatin (*cis*-diamminedichloroplatinum(II)) is the first metal-based anti-cancer drug. The discovery of cisplatin *cis*-[Pt^{II}(NH₃)₂Cl₂] was a defining moment that triggered our interest in platinum(II) and other metal-containing complexes as potential novel anticancer drugs¹.

The four main steps in the mechanism of action of cisplatin that lead to cell survival or apoptosis are as follows; (i) cellular uptake, (ii) aquation/activation, (iii) DNA platination, and (iv) cellular processing of Pt-DNA lesions². Passive diffusion was initially thought to play a significant role in the uptake of cisplatin³. It was also thought that passive diffusion was embedded in SARs through the requirement of charge neutrality. Recently, active transport *via* the copper transporters CTR1 and CTR2 has been implicated as the major route of platinum access to the cell⁴.

Leaving groups, such as chloride in cisplatin and oxalate in oxaliplatin, can modify the kinetics of hydrolysis as well as reactivity of the drug⁵. Some aquated/activated platinum complexes can react with the N7 positions of guanosine and adenosine residues. The platinum center can coordinate to guanine bases from different DNA strands to form intrastrand cross-

links such that the major intrastrand dGpG cross-link induces a significant distortion in the DNA double helix⁶. The DNA lesion is then distinguished by cellular machinery that can either repair the lesion, bypass it or initiate apoptosis. The most important mechanism by which classical platinum complexes are believed to induce apoptotic cell death is inhibition of transcription. When RNA polymerases transcribe DNA, they stall at the platinum cross-link and recruit transcription-coupled reparation machinery. If this machinery is unable to repair the lesion then programmed cell death is evoked⁴.

QSAR models are mathematical equations, which construct a relationship between chemical structures and biological activities. Also, these models have the ability to provide a deeper knowledge about the mechanism of biological activity. Finding a set of molecular descriptors with higher impact on the biological activity of interest⁷⁻¹⁰ is the first step of a typical QSAR study. In the QSAR modeling, a wide range of descriptors has been used. These descriptors have been classified into different categories, such as constitutional, geometrical, topological, quantum chemical and so on. There are several variable selection models such as multiple linear regression

(MLR), simulated Annealing algorithm (SA)^{11,12}, genetic algorithm (GA)¹³, partial least squares (PLS), and so on⁹⁻¹⁴. MLR yields models are simpler and easier to interpret than PLS, owing to the fact that they perform regression on latent variables and do not have physical meaning. The quantitative structure-activity relationship studies (QSAR)^{15,16} is one of the most effective computational approaches for the inspection of inhibition mechanism.

In the present study, multiple linear regressions (MLR), simulated annealing (SA), genetic algorithm (GA) and artificial neural networks (ANN) were applied as linear and non-linear approaches to investigate the QSAR¹⁷ in Platinum (II) Anticancer drugs with N-donor ligands. QSAR models have also been used to select more effective descriptors to obtain a hybrid computational model for a rough prediction of the inhibitory activity of Pt(II) complexes. The ability of these methods in predicting the inhibitory activity of Platinum (II) complexes have also been compared.

Methods

Geometry optimizations of Platinum compounds were carried out using the B3lyp/lan12dz at the Gaussian 03W (Ref 18). Different types of numerical descriptors were generated to describe each compound. These descriptors were categorized in topological, geometrical, MoRSE^{19,20}, RDF^{20,21}, GETAWAY^{22,23}, auto-correlations²⁰ and WHIM^{24,25} groups. The molecular descriptors for constructing the best model were calculated using the Dragon program²⁶. In total, 3226 descriptors were generated.

The number of descriptors was then reduced through an objective feature selection in three steps. At first, descriptors that had the same value for at least 70% of compounds in the dataset were removed. In the next step, the descriptors with correlation coefficient less than 0.25 with the dependent variable ($-\log IC_{50}$) were considered redundant and removed²⁷. After these two steps, the number of descriptors was reduced to 1279. A stepwise multiple linear regression procedure based on the forward-selection and backward-elimination methods was used for the inclusion or rejection of descriptors in the QSAR models. High correlation coefficient (R), low standard deviation, least numbers of independent variables, high ability to predict and high F statistic value²⁸ are necessary for an ideal model.

The ANN was developed as a generalization of mathematical method of human cognition and neural biology.

The connections between neurons created the network function, each connection between two neurons had a weight coefficient attached to it. Therefore, the standard network structure for function approximation is the multiple layer perceptron with one or more hidden layers followed by an output layer. Multiple layers of neurons with non-linear transfer functions allow the network to learn non-linear and linear relationships between input and output vectors. The number of input and output variables in the process under investigation (Figure 1) determined the number of neurons in the input and output layers.

The neurons in the hidden layer had a bias, b , which was added with the weighted inputs to form the neuron input:

$$n_i = b_i + \sum_{j=1}^m (W_{in}(j,i) * In_j), i = 1, 2, \dots, N'$$

Where m and N' are the number of inputs and the number of neurons in the hidden layer, respectively. The transfer function of the hidden layer (f) acts on n to obtain the outputs of each neuron in the hidden layer:

$$a_i = f(n_i)$$

The network output is given in the following equation:

$$out = f'(b_{out} + (i) * a_i), i = 1, 2, \dots, N'$$

Where, f' is the transfer function for the output layer.

The best subset of descriptors selected in MLR was fed into the neural networks with three-layer feed-forward in the MLR-ANN method. Such networks may identify the non-linear relationship between the structural descriptors and inhibitory activity of compounds that were trained using TSET members with the Levenberg-Marquart algorithm²⁹.

In the SA-ANN and GA-ANN methods, 1279 descriptors were considered as possible input of the ANN and were fed into the input layer (Figure 2).

Root mean square error was calculated using the following equation:

$$RMSE = \sqrt{\frac{\sum_{i=1}^n (y_i - y_o)^2}{n}}$$

Where y_i is the desired output, y_o is the predicted value by model, and n is the number of molecules in this study's data set. All calculations in this study were carried out in Matlab environment (V 7.12, The Mathworks, Inc).

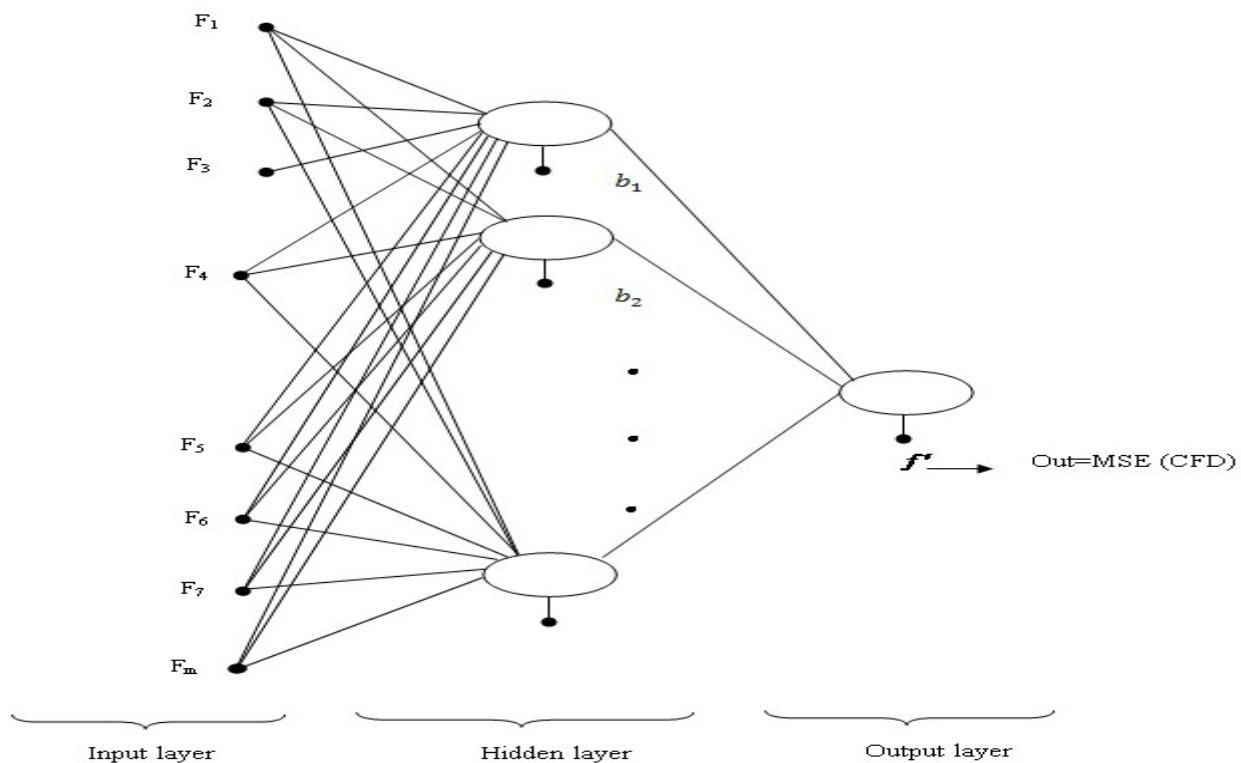


Figure 1 — The neural network model

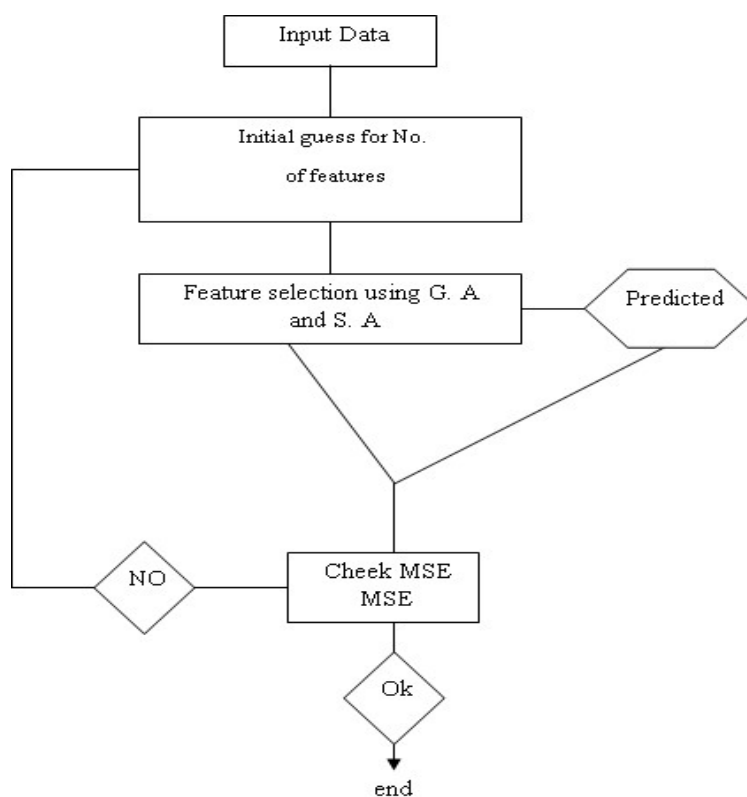


Figure 2 — The employed procedure for finding optimum descriptors of the ANN models

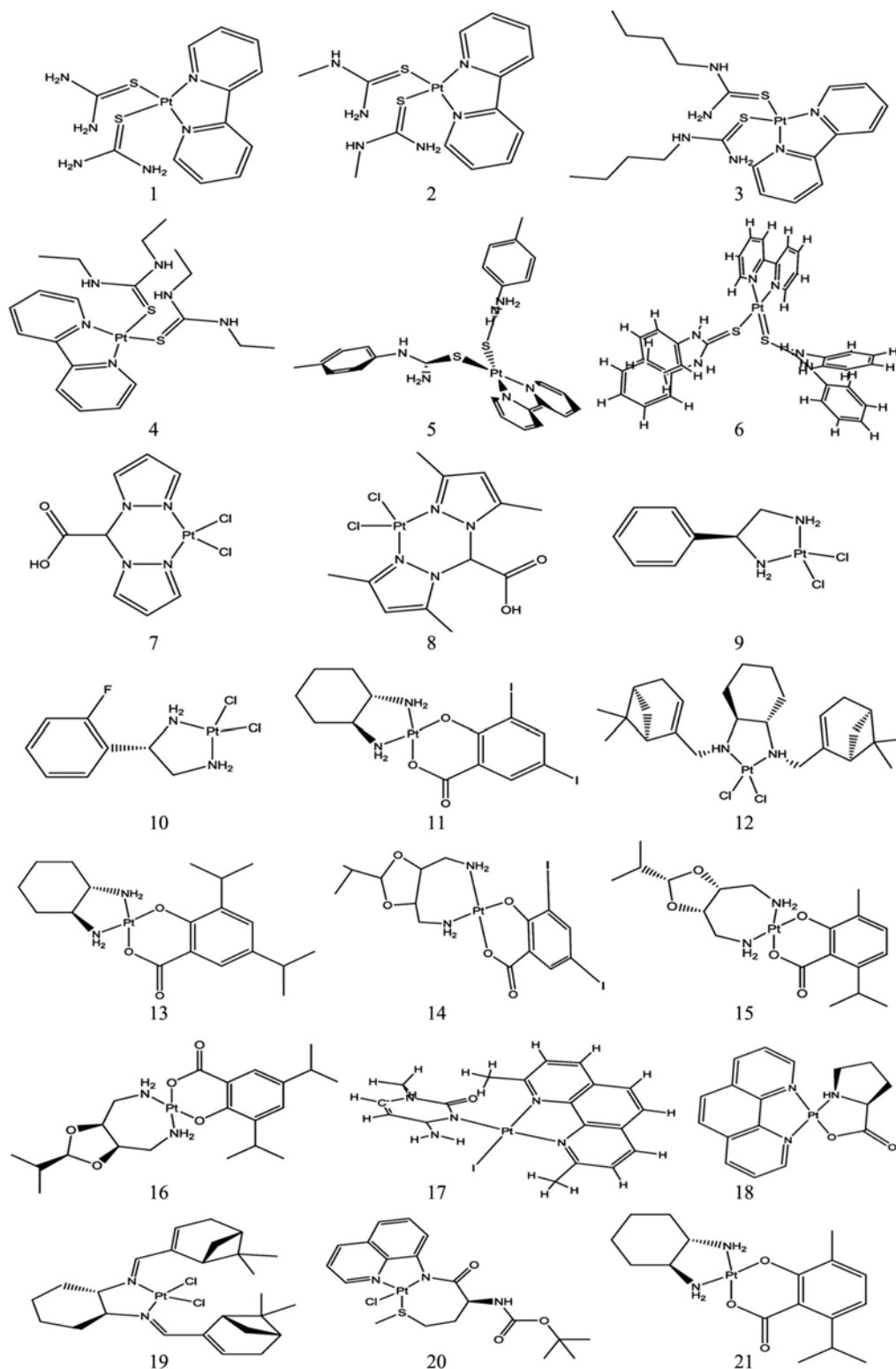


Figure 3 - Optimized structure of the platinum complex used to build QSAR models with B3lyp/lanl2dz

Results and Discussion

The studied platinum complexes are shown in Figure 3. The optimized geometries of the Pt(II)

complexes are shown in Table I and Table II. The optimized geometries of the complexes have square planar configuration with angles close to the ideal values

Table I — Optimized bond length (Å) and energies(Kcal/mol) of Platinum drug complexes in the B3lyp/lan12dz

Compd	Pt-S	Pt-O	Pt-Cl	Pt-I	Pt-N	-log(IC ₅₀)	E Kcal/mol
1	2.45				2.07	-0.267	-584505.587
	2.45				2.08		
2	2.45				2.07	-0.344	-633684.629
	2.44				2.07		
3	2.44				2.07	-0.06	-781241.773
	2.44				2.07		
4	2.44				2.07	-0.057	-781229.261
	2.44				2.07		
5						-0.301	-922652.397
6					2.07	-0.176	-1162593.770
					2.07		
7			2.39		2.05	-0.176	-518073.749
			2.39		2.05		
8			2.39		2.07	-0.602	-616451.851
			2.40		2.07		
9			2.41		2.09	-0.580	-357029.294
			2.40		2.09		
10			2.40		2.09	-0.491	-419115.715
			2.40		2.09		
11		1.99			2.10	-0.188	-614397.381
		2.00			2.09		
12		1.99	2.41		2.12	-0.222	-797300.925
		1.99	2.41		2.10		
13		1.99			2.11	-0.553	-748458.456
		2.00			2.10		
14		1.99			2.10	-0.334	-757672.918
		2.00			2.10		
15		2.00			2.10	-0.104	-842547.445
		2.00			2.10		
16		2.00			2.10	-0.255	-891733.994
		1.99			2.10		
17				2.70	2.06		
					2.11	-0.041	-759978.880
					2.07		
18		2.00			2.09	-0.991	-682579.022
					2.07		
					2.03		
19			2.41		2.05	0.155	-796384.671
			2.41		2.05		
20	2.45		2.45			-0.740	-796134.181
21		2.00			2.10	-0.173	-699270.218
		2.00			2.10		

of 90 and 180. The calculated Pt-Cl, Pt-N, Pt-S and Pt-O bond lengths were 2.39-2.41, 2.03-2.11, 2.44-2.45 and 1.99-2.00 Å, respectively in accordance with their experimental values³⁰⁻³³. The optimized bond angles are shown in Table II.

The SPSS³⁴ software was used for MLR model processing and among the obtained models, the best was selected as shown in Table III. The RMSE in MLR-MLR for predicted activity was found to be 0.1273 in the gas phase. Also, the correlation coefficient (R²) calculated for the PSET was 0.763 in the gas phase.

The descriptors, which were selected using the MLR-MLR method, were fed into the neural networks to establish the MLR-ANN model. In this model, the RMSE for predicted activity and compounds were found to be 0.0129 in the gas phase.

The best selected descriptors using MLR-MLR and MLR-GA, SA-ANN and GA-ANN methods are shown in Tables III-VII.

G2u (Tables III and IV), E3e (Table III) and E3u (Table IV) and G2e (Table VI) are the global WHIM descriptors that represent the total size, and can

Table II — Optimized bond Angle (\AA) of Platinum drug complexes in the B3lyp/lanl2dz

Compd	N-Pt-N	S-Pt-S	S-Pt-S	Cl-Pt-Cl	O-Pt-O	I-Pt-N	N-Pt-O	Cl-Pt-S
1	79.92	86.38	86.38					
2	79.88	87.78	87.78					
3	79.84	88.57	88.57					
4	79.71	85.36	85.36					
5	79.91	77.38	77.38					
6	79.76	88.81	88.81					
7	89.45			92.99				
8	86.49			91.22				
9	84.50			98.05				
10	84.55			98.02				
11	84.16				95.2587			
12	82.59			94.17				
13	83.89				95.54			
14	103.56				96.38			
15	103.06				94.97			
16	103.07				96.76			
17	80.01					83.9482		
18	80.88						83.1248	
19	79.52			89.27				
20	80.80							84.1184
21	83.83				92.68			

Table III — The best selected descriptors using MLR-MLR method

Descriptor	Definition	Type
E3e	3 rd component accessibility directional WHIM index/ weighted by atomic sanderson electronegativities	WHIM descriptors
G2u	2st component symmetry directional WHIM Index/unweighted	WHIM descriptors
R5m+	R maximal autocorrelation of lag 5/weighted by atomic masses GETAWAY descriptors	GETAWAY descriptors

Table IV — The best selected descriptors using MLR-GA method

Descriptor	Definition	Type
G2u	2st Component symmetry directional WHIM index/unweighted	WHIM descriptors
E3u	3 rd component accessibility directional WHIM index/unweighted	WHIM descriptors
D/Dr03	Distance/detour ring index of order 4	Topological descriptors

independently play a significant role in the modeling of measured directions and produce the simpler models^{24,25}. These kinds of descriptors are built in such a way as to capture relevant molecular 3D information on molecular size, shape, and symmetry as well as atom distribution with respect to invariant references frames.

GETAWAY (Geometry, Topology, and Atom-Weights Assembly) descriptors^{33,22,23} encoded the geometrical information obtained from the molecular matrix, the topological information obtained from the molecular graph and the information obtained from atomic weights. These descriptors have been specially designed with the aim of matching the 3D-molecular geometry and each of the calculated descriptor is R5m+ (Table III).

The 3D-MoRSE descriptors^{19,20}, such as Mor17m (Table IV) and Mor09v (Table VI), were obtained

through the molecular transformation employed in the electron diffraction studies. The electron diffraction did not directly result in atomic coordinates, but allows the diffraction patterns from which the atomic coordinates are derived by mathematical transformations. To establish relationships between molecular structure and physical, chemical or biological properties the 3D MoRSE code was used.

Tables IV and V show that the descriptors used were topological descriptors, such as Jhetz and D/Dr03. The topological index mathematically encoded information regarding the structure of molecules, which have been depicted as graphs. Molecular graph are sensitive to size, shape, branching, cyclicity and, to a certain extent, the electronic characteristics of molecules²⁰.

VED1 (Table V) is an eigenvalue based indices descriptor. The Eigenvalue Sum Descriptors are

Table VI — The best selected descriptors using G.A-ANN method

Descriptor	Definition	Type
Mor09v	Signal 09/weighted by atomic van der waals volumes	3D-MoRSE descriptors
RDF140v	Radial Distribution function 140/weighted by atomic van der waals volumes	RDF descriptors
G2e	2 st component symmetry directional WHIM index /weighted by atomic sanderson electronegativities	WHIM descriptors

Table V — The best selected descriptors using S.A-ANN method

Descriptor	Definition	Type
Jhetz	Balaban-type index from z weighted distance matrix(Barysz matrix)	Topology descriptors
VED1	Eigenvector coefficient sum from distance matrix	Eigenvalue-based indices
Mor17m	Signal 17/weighted by atomic masses	3D-MoRSE descriptors

Table VII — Statistical parameters of different QSAR models

QSAR Models	RMSE R ²
MLR-MLR	0.12737 0.763
MLR-ANN	0.0129 0.819
SA-ANN	0.01060 0.847
MLR-GA	0.0125 0.825
GA-ANN	0.0099 0.904

Table VIII — Observed and predicted values of -logIC50 using GA-ANN

Compd	Observed	Predicted
1	-0.267	-0.31698
2	-0.344	-0.1758
3	-0.061	-0.19146
4	-0.057	0.002802
5	-0.301	-0.23683
6	-0.176	-0.05305
7	-0.176	-0.25251
8	-0.602	-0.44432
9	-0.58	-0.54826
10	-0.491	-0.48697
11	-0.188	-0.10904
12	-0.222	-0.20943
13	0.553	0.534929
14	-0.335	-0.29695
15	-0.104	-0.18324
16	-0.255	-0.29824
17	-0.041	-0.04863
18	-0.991	-0.97913
19	0.222	-0.06093
20	-0.74	-0.74487
21	-0.173	-0.08284

Table IX — Descriptor values for GA-ANN model

Factor 1	Factor2	Factor3
Mor 9v	RDF140V	G2e
-1.021	0	0.161
-0.769	0	0.156
-0.697	0.816	0.163
-1.018	0	0.144
-1.34	2.127	0.151
6.446	0	0.144
-1.308	0	0.19
-0.654	0	0.161
-0.459	0	0.235
-0.526	0	0.201
-1.024	0.513	0.161
0.159	1.351	0.148
-0.651	0.592	0.147
-0.911	1.689	0.176
-0.553	1.246	0.155
-0.573	3.175	0.151
-0.933	0	0.153
-0.991	0	0.173
-0.394	0	0.146
-0.008	0.354	0.159
-0.428	0.005	0.151

computed from Weighted Distance Matrices of a Hydrogen-depleted Molecular Graph²⁰.

RDF descriptors^{20,21} are a molecular descriptor that uses the 3D coordinates of the atoms in a molecule to describe the probability distribution of distances in a three-dimensional molecule and one of these descriptors is RDF140v as shown in Table VI. These descriptors are independent of the atom number such as size of a molecule.

Molecular descriptors giving the best linear models were used as network inputs in the MLR-ANN method and the activities as target outputs.

The 1279 descriptors were fed to the SA-ANN, MLR-GA and GA-ANN models, the best parameters which could minimize the value of fitness function were

selected using SA and GA. The statistical parameters of all QSAR models are shown in Table VII. In the GA-ANN model, the RMSE and R-square were calculated as 0.0099 and 0.904, respectively in the gas phase, therefore, the GA-ANN model was determined as better than the other models and as such, only the descriptors used in this model were evaluated.

The GA-ANN method was utilized to calculate the results of the GA-ANN model with 3 input parameters (Table VI). The observed and predicted values of -logIC50 using GA-ANN method and the value of the selected descriptors using GA-ANN model are shown in Table VIII and Table IX respectively. The plot showing the variation of observed *versus* predicted log IC50 values, using the GA-ANN method is shown in Figure 4.

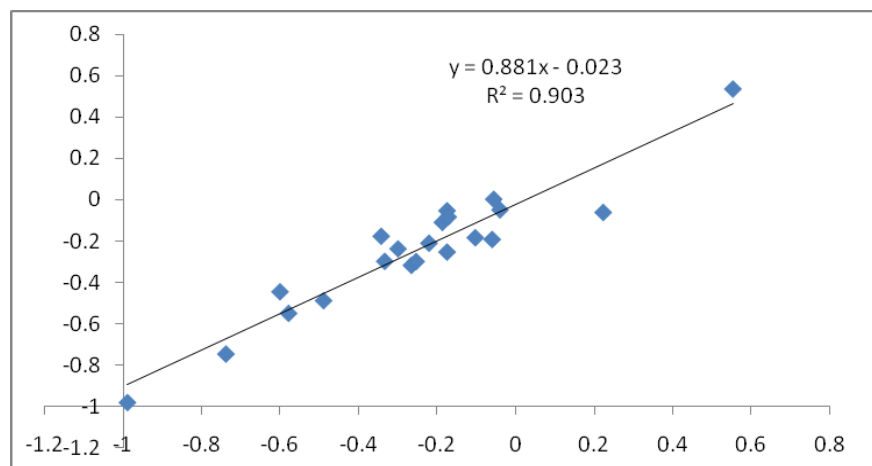
Figure 4 — Plot between observed and predicted $-\log(\text{IC}_{50})$ using GA-ANN model

Table X — Test and valid series in QSAR models*

QSAR Models	Test Series	Valid Series
MLR-ANN	15,16	1,3,14
GA-MLR	6,8	19,20
SA-ANN	7,8	12,13,15
GA-ANN	11,18	13,17,20

* The naming are according to Figure 3

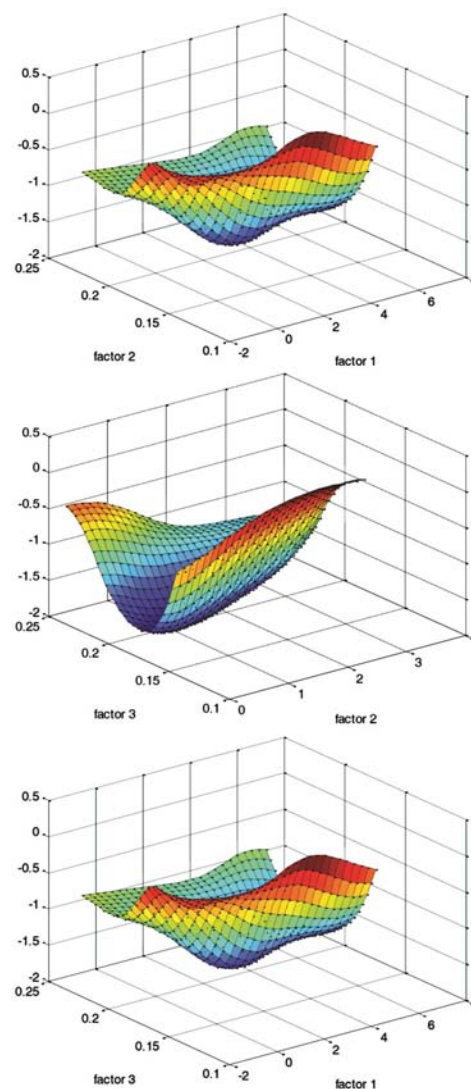
In GA-ANN, SA-ANN, MLR-ANN, MLR-GA methods, 80%, 10% and 10% of data sets were randomly chosen as training, validation and test sets, respectively. Table X shows test and valid series in QSAR models in Pt(II) compounds

The two-dimensional plots of the Mor9v (factor 1), RDF140v (factor 2) and G2e (factor 3) descriptors (Table VIII and Table IX) versus $-\log(\text{IC}_{50})$ Experimental (R) were plotted using the Matlab environment (V 7.12, The Mathworks, Inc, Figure 5). It was shown that factors 1 and 2, 1 and 3, and 2 and 3 were also affected. For the average values of the 1 and 3, and 2 and 1 factors, the $-\log(\text{IC}_{50})$ experimental was minimal. While for the least values of the 2 and 3 factors, the $-\log(\text{IC}_{50})$ experimental was maximum.

With an increase in the empirical negative logarithm half maximal inhibitory concentration ($-\log(\text{IC}_{50})$) the amount of empirical half maximal inhibitory concentration (IC_{50}) was reduced.

Table VIII showed that 13,19,17 compounds were the best drugs. They had high empirical negative logarithm half maximal inhibitory concentration.

Descriptors were selected using GA-ANN method and employed to build the final model. Thus Mor9v, RDF and G2e descriptors were the most important. These descriptors are shown in Table VI.

Figure 5 — Two-dimensional plot of the Mor9v, RDF140v and G2e descriptors (Factor 1, Factor 2, Factor 3) versus $-\log(\text{IC}_{50})$ experimental (R_1)

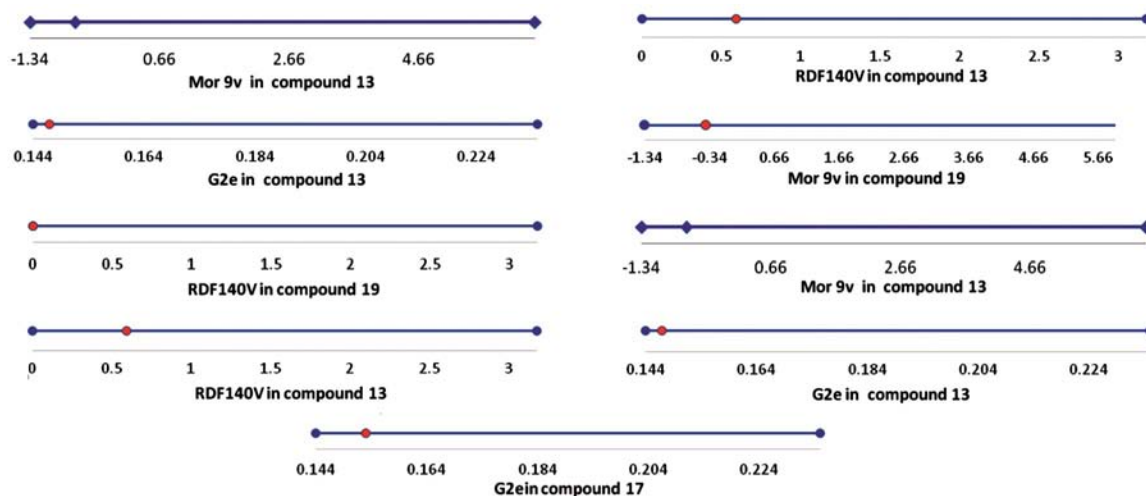


Figure 6 — Plot Mor 9v, RDF140v, G2e in 13,19,17 compounds in GA-ANN model

The graphs Mor09v, RDF and G2e descriptors in minimum and maximum values of 13,17,19 compounds were plotted using excel program (Figure 6). It was shown that in 13,19,17 compounds, values for descriptors were at the minimum.

Thus this work predicts in new design for this class of drugs the Mor09v, RDF and G2e descriptors values are the minimum and the weak ligands such as chloride, iodide, oxalate as leaving group coordinated with Platinum (II) with N-donor ligands.

Conclusions

Although a large number of non-linear and hybrid methods could be employed to establish the QSAR models, the GA-ANN model is admittedly one of the best. This can be attributed to the complicated relationships between the structure and activity of the Pt(II) compounds. These results also proved that Mor9v, RDF140v and G2e descriptors were more significant than other descriptors in building this QSAR model and predicting the biological activity of Platinum substitution patterns.

Acknowledgement

The authors gratefully acknowledge the support provided by the Islamic Azad University of Rasht.

References

- 1 Frezza M, Hindo S, Chen D, Davenport A, Schmitt S, Tomco D & Ping Dou Q, *Curr Pharm Des*, 16 (2010) 1813.
- 2 Johnstone T C, Park G Y & Lippard S J, *Anticancer Res*, 34 (2014) 471.
- 3 Johnstone T C, Suntharalingam K & Lippard S J, *Chem Rev*, 116 (2016) 3436.
- 4 Howell S B, Safaei R, Larson C A & Sailor M J, *Mol Pharmacol*, 77 (2010) 887.
- 5 Silva H, Barra C V, Rocha F V, Frederic Frézard F, Lopes M T P & Fontes A P S, *J Braz Chem Soc*, 21 (2010) 1961.
- 6 Maalina J, Hofr C, Maresca L, Natile G & Brabec V, *Biophysical Journal*, 78 (2000) 2008.
- 7 Ojha L K, Sharma R & Bhawsar M R, *Int J Res Biosciences*, 2 (2013) 1.
- 8 Garkani-Nejad Z & Saneie F, *Bull Chem Soc Ethiop*, 24 (2010) 317.
- 9 Doreswamy & Vastrad C M, *J Adv Bioinformatics Appl Res*, 3 (2012) 379.
- 10 Taxak N & Bharatam P V, *Indian J Pharm Sci*, 76 (2013) 680.
- 11 Rasdi Rere L M, Ivan Fanany M & Arymurthy A M, *Procedia Computer Science*, 72 (2015) 137.
- 12 Gomes A I, Pires J C, Figueiredo S A & Boaventura R A, *Environ Technol*, 35 (2014) 945.
- 13 Bagheban Shahri F, Niazi A & Akrami A, *J Mex Chem Soc*, 59 (2015) 203.
- 14 Kiyoshi Hasegawa K, *Curr Comput Aided Drug Des*, 1 (2010) 24.
- 15 Valadkhani A, Asadollahi-Babolib M & Mani-Varnosfaderanic A, *J Braz Chem Soc*, 26 (2015) 619.
- 16 Tomal J H, Welch W J & Zamar R H, *J Chem Inf Model*, 56 (2016) 501.
- 17 Mansourian M, Saghaie L, Fassihi A, Madadkar-Sobhani A & Mahnam K, *Med Chem Res*, 22 (2013) 4549.
- 18 DeMelo E B & Ferreira M M, *Eur J Med Chem*, 44 (2009) 3577.
- 19 Devinyak O, Havrylyuk D & Lesyk R, *J MolGraphics Modeling*, 54 (2014) 194.
- 20 Todeschini R & Consonni V, *Handbook of Molecular Descriptors* (Wiley-VCH Verlag GmbH, Weinheim) (2000).
- 21 Jagiello K, Sosnowska A, Kar S, Demkowicz S, Daško M, Leszczynski J, Rachon J & Puzyn T, *Struct Chem* (2017) 1-16. DOI: 10.1007/s11224-016-0903-x
- 22 Rojas C, Ballabio D, Consonni V, Tripaldi P, Mauri A & Todeschini R, *Theoretical Chemistry Accounts*, 135 (2016) 1.
- 23 Jukic M, Rastija V, Opacak-Bernardi T, Stolic I, Krstulovic L, Bajic M & Glavas-Obrovac L, *J Mol Str*, 1133 (2017) 66.

- 24 Gramatica P, *QSAR Comb Sci*, 25 (2006) 301.
- 25 Li F, Liu J & Cao L, *Emerging Contaminants*, 1 (2015) 8.
- 26 Todeschini R, *Milano Chemometrics QSAR Group*, <http://www.disat.unimib.it/chem> (2000).
- 27 Nirouei M, Ghasem G, Abdolmaleki P, Tavakoli A & Shariati S, *Indian J Biochem Biophys*, 49 (2012) 202.
- 28 Yousefinejad S, Honarasa F & Chaabi M, *New J Chem*, 12 (2016) 40.
- 29 Ghaffari A, Khodayari A R & Arefnezhad S, *Int J Automotive Engineering*, 6 (2016) 2256.
- 30 Oliveira P A S, Sartori L M, Rey N A, Santos D H F, De Oliveira M A L & Costa L A S, *J Braz Chem Soc*, 24 (2013) 1732.
- 31 Varbanov H P, Jakupec M A, Roller A, Jensen F, Galanski M & Keppler B K, *J Med Chem*, 56 (2013) 330.
- 32 Kolay S, Wadawale A, Nigam S, Kumar M, Majumder C & Jain V K, *Inorg Chem*, 54 (2015) 11741.
- 33 Ilavarasi R, *Der Chemica Sinica*, 7 (2016) 70.
- 34 SPSS, Version 19 (2010) available at <http://www.spss.com>.